SEISMIC PERFORMANCE AND CRACK PATTERN OF CONCRETE BLOCK INFILLED RC FRAMES

Ho CHOI[1], Yoshiaki NAKANO[2] and Yasushi SANADA[3]

ABSTRACT: The objective of this study is to develop pre- and post-earthquake seismic evaluation method of concrete block infilled reinforced concrete frames. For this purpose, full-scale, one-bay, single-story specimens having different axial loads in columns and different opening configurations in wall are tested to investigate typical school buildings in Korea. In this paper, the relationship between observed damage and seismic performance primarily focusing on crack width in concrete block walls, load bearing capacity, and residual deformation is discussed.

Key Words: concrete block (CB) wall, reinforced concrete frame, damage assessment, residual seismic capacity, crack width

INTRODUCTION

In some regions of Asia, Europe, and Latin America where earthquakes frequently occur, serious earthquake damage is commonly found resulting from catastrophic building collapse. Such damaged buildings often have unreinforced masonry (URM) walls, which are considered non-structural elements in the structural design stage, and building engineers therefore have paid less attention to their effects on structural performance although URM walls may interact with boundary frames as has been often found in the past damaging earthquakes.

After an earthquake, the major concerns to damaged buildings are their safety/risk to aftershocks, quantitative damage assessment to evaluate their residual seismic capacity and to identify necessary actions on the damaged buildings. Post-event damage evaluation is therefore essential for quick recovery of damaged community as well as pre-event seismic evaluation and strengthening of vulnerable buildings. Few investigations on masonry walls, however, have been made to quantitatively identify their damage level and criteria to judge necessary actions for their continued use, repair and rehabilitation.

In this study, concrete block (CB) infilled reinforced concrete frames for school buildings in Korea, where CB walls are typically unreinforced, are experimentally investigated to develop pre- and post-earthquake seismic evaluation method. In the tests, full-scale, one-bay, single-story specimens having different axial loads in columns and different opening configurations in walls are tested under cyclic loading, and the contribution of URM walls to overall behaviors and crack patterns and widths in walls and frames which may be of great significance for post-event assessment are carefully observed.

In this paper, the relationship between observed damage and seismic performance primarily focusing on crack width in concrete block walls, load bearing capacity, and residual deformation is discussed.

---

[1] Graduate student, Graduate School of Engineering, The University of Tokyo
[2] Associate professor, Institute of Industrial Science, The University of Tokyo, Dr. Eng.
[3] Research Associate, Earthquake Research Institute, The University of Tokyo, Dr. Eng.

OUTLINE OF EXPERIMENT

Test Specimen

Figure 1 shows a standard design for Korean school buildings in the 1980s [1]. As can be found in this figure, unreinforced concrete block (CB) walls are commonly used as partition walls or exterior walls in Korean school buildings. In this study, 4 specimens representing a first or fourth story of 4 story RC school buildings are tested under cyclic loading. They are infilled wall type 1 (IW1) assuming a first story, infilled wall type 2 (IW2) assuming a fourth story, and wing wall type (WW) and partial height wall type (PW) both having opening in wall. The axial force applied in each column is 720 kN (4 N/mm^2) for specimens IW1, WW, and PW while 180 kN (1 N/mm^2) for IW2.

The design details of specimen IW1 are shown in Figure 2. Since seismic design provisions for buildings were introduced in 1988 in Korea, the model structures studied herein are not designed to seismic loads. Therefore, they have (1) large spacing of hoops (300 mm) and (2) 90 degree hook at both ends of hoops as shown in the figure. Specimens IW1, WW, and PW have identical re-bar arrangement in columns but different wall arrangement, while IW2 has fewer re-bars than other 3 specimens. Concrete block units are laid in the RC frame after concrete is hardened. All specimens are fabricated and tested at RIST (Research Institute of Industrial Science and Technology) in Korea to follow the Korean construction practice.

Material Characteristic

Material test results are shown in Tables 1 through 3 (the average values of three samples are shown in Tables). Although the design strength of concrete specified in the standard design of Korean school buildings in the 1980s is 21 N/mm^2, the compressive strength of test pieces exceeds the design value as shown in Table 1. The deformed bar SD40 (nominal yield strength: 395 N/mm^2) is used for longitudinal and shear reinforcement. The size of a CB unit is 390×190×190 mm. It has three hollows inside and a half-sized hollow on both ends as shown in Figure 2. Joint mortar having the cement-to-sand ratio of 1:3.5, which is generally used in Korea, is placed horizontally and vertically between CB units in wall when they are laid and set in the RC frame.
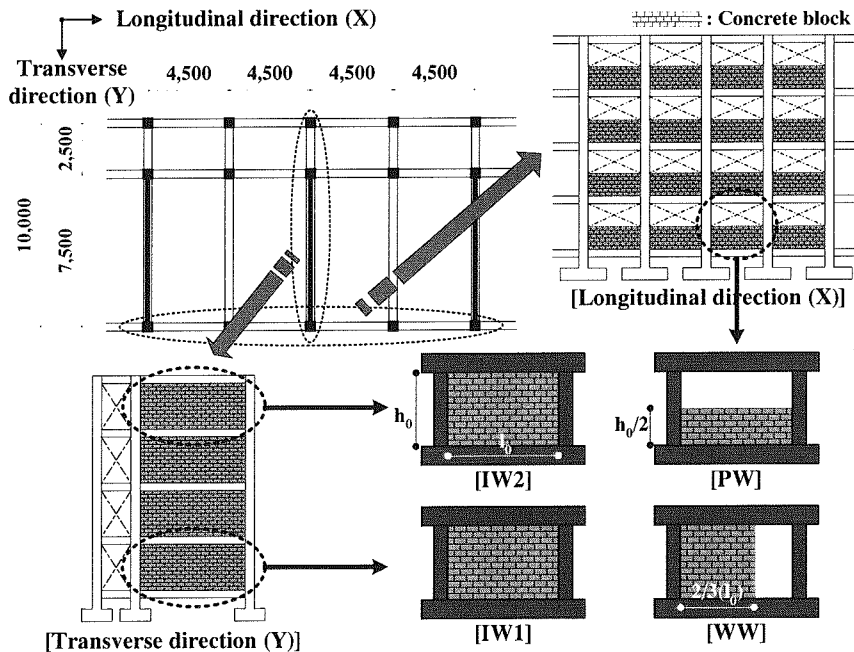

Figure 1. Standard design of Korean school buildings in the 1980s and specimen configuration

Test Setup and Test Program

Figures 3(a) through (e) show the fabrication process of specimens and the test setup. The fabrication of specimens and concrete casting are both made horizontally as shown in Figures 3(a) and (b). After concrete is hardened, the specimens are reinforced with steel angles bolted at the upper and lower stubs to prevent crack development in columns, and then they are erected as shown in Figure 3(c). CB
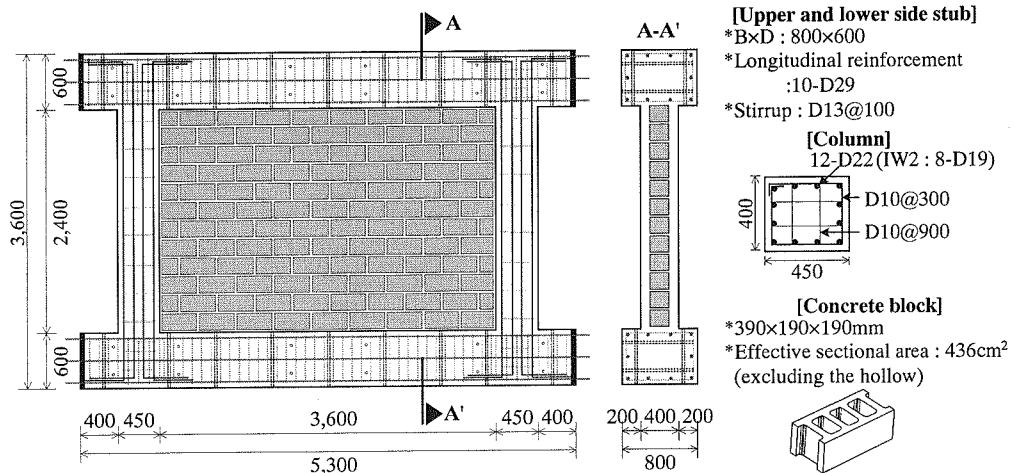

[Upper and lower side stub]
*B×D : 800×600
*Longitudinal reinforcement
     :10-D29
*Stirrup : D13@100

[Column]
12-D22 (IW2 : 8-D19)
D10@300
D10@900
450

[Concrete block]
*390×190×190mm
*Effective sectional area : 436cm²
(excluding the hollow)

Figure 2. Detail of specimen (IW1)

Table 1. Mechanical properties of concrete

Specimen	Compressive strength (N/mm²)	Young's modulus (N/mm²)	Split tensile strength (N/mm²)	Specimen	Compressive strength (N/mm²)	Young's modulus (N/mm²)	Split tensile strength (N/mm²)
IW1	27.3	2.28×10^4	2.4	WW	23.8	2.11×10^4	2.0
IW2	29.6	2.30×10^4	2.4	PW	26.1	2.03×10^4	2.2

Table 2. Mechanical properties of reinforcement

Bar	Use / Member	Yield strength (N/mm²)	Tensile strength (N/mm²)	Young's modulus (N/mm²)
D10	Hoop / Column	404	581	1.91×10^5
D13	Stirrup / Stub	419	622	1.88×10^5
D19	Longitudinal reinforcement of IW2 / Column	432	599	1.95×10^5
D22	Longitudinal reinforcement of IW1, WW, PW / Column	498	598	1.88×10^5
D29	Longitudinal reinforcement / Stub	455	-*	2.09×10^5

* strain not measured due to displaced gauge

Table 3. Mechanical properties of concrete block and joint mortar

| Concrete block				Joint mortar***	
Block unit*		Block prism**			
Compressive strength (N/mm²)	Young's modulus (N/mm²)	Compressive strength (N/mm²)	Young's modulus (N/mm²)	Compressive strength (N/mm²)	Young's modulus (N/mm²)
15.9	3.60×10^4	10.3	2.21×10^4	20.5	1.30×10^4

* excluding hollow areas   ** 3 layered specimen   *** cylinder type
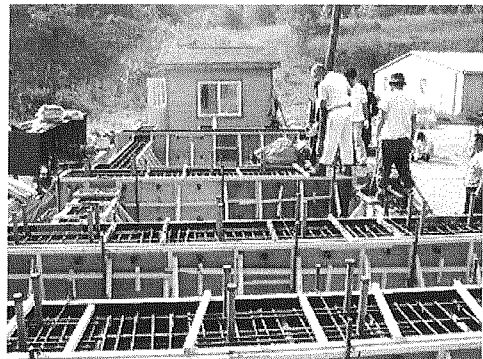
units are laid and set with mortar in the testing laboratory as shown in Figure 3(d). Each specimen is finally placed in the testing frame and loading jacks are set as shown in Figure 3(e).
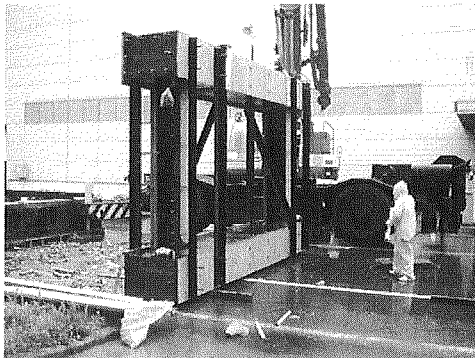
Cyclic lateral loads are applied to each specimen through a loading beam tightly fastened to the
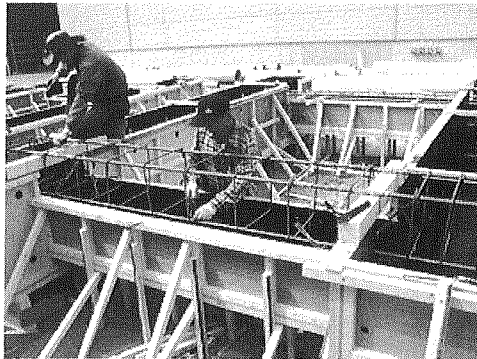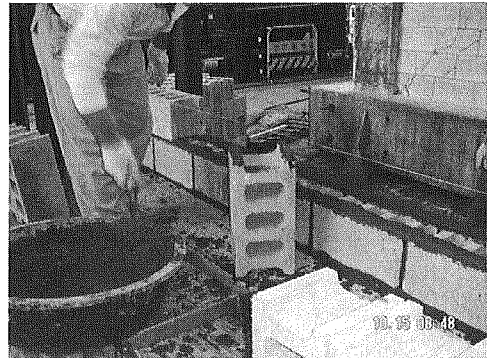

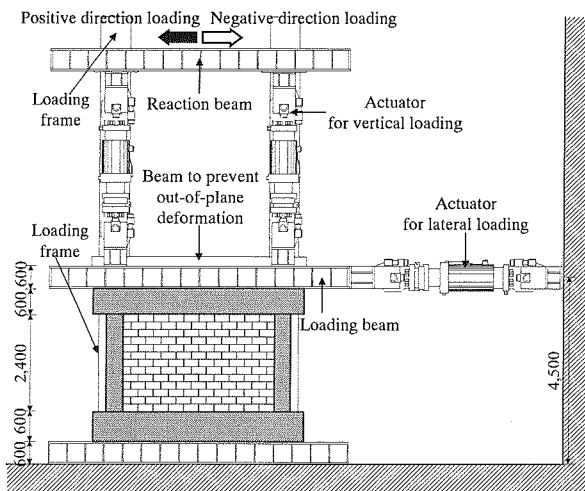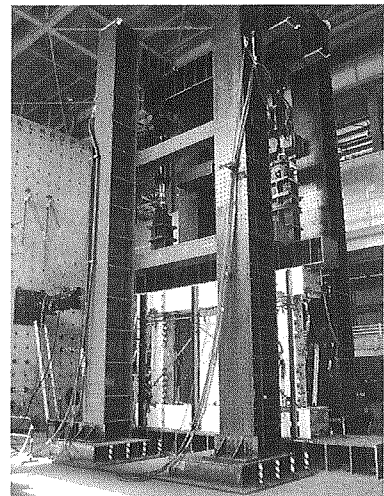(a) Reinforcement arrangement

(b) Horizontal concrete casting

(c) Erection

(d) CB wall setting

(e) Test setup

Figure 3. Fabrication of specimen and test setup

specimen. Figure 4 shows the loading history, where a peak drift angle R is defined as "lateral displacement (δ_p) / column height (=2,400 mm)". As shown in the figure, peak drift angles of 0.1, 0.2, .0.4, 0.67, 1.0, and 2.0% are planned and 2.5 cycles for each peak drift are imposed to eliminate one-sided progressive failure (unsymmetric failure pattern in positive or negative loadings). It should also be noted that 0.4% loading is imposed after 1.0% to investigate the effect of small amplitude loading after large deformation (i.e., aftershocks). After severe damage is found, the specimen is pushed over to collapse. A constant axial load of 1,440 kN (720 kN for each column) is applied to specimens IW1, WW and PW while 360 kN (180 kN for each) to specimen IW2.

The measurement system is shown in Figure 5. The relative lateral displacement between upper and lower stub, the vertical displacement of each column, and the diagonal deformation of frame and CB wall are measured. To measure the curvature distribution along column, displacement transducers are attached on both sides of each column at an interval of 150 mm (600 mm in the mid-column). Strains on major portions of longitudinal and shear reinforcement in columns are measured. In order to calculate the axial force carried by the CB wall, strain gauges are attached on both surfaces of 3 units in the uppermost layer immediately below the upper stub. The relation between axial stress and strain is pre-determined from material testing of CB unit. From this result and strains measured during the experiment, the axial stress in CB wall is calculated. Maximum crack widths at peak loads and residual crack widths at unloaded stages are carefully measured in RC columns and CB wall.

TEST RESULTS

Failure Patterns
Figure 6 shows the crack pattern of each specimen at the first cycle with peak drift angle of +1.0%, which may facilitate to understand the resistance mechanism in the specimens. It should be noted that the specimens finally fail during the subsequent loading stage with larger amplitude. The failure pattern observed in each specimen is briefly described subsequently.
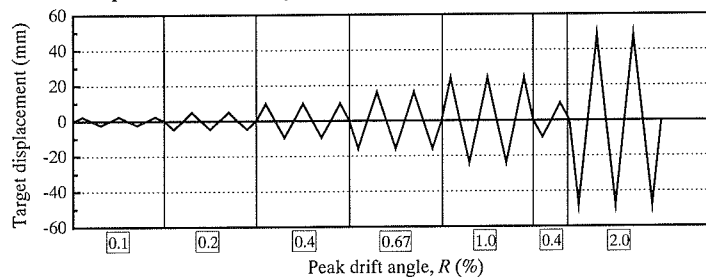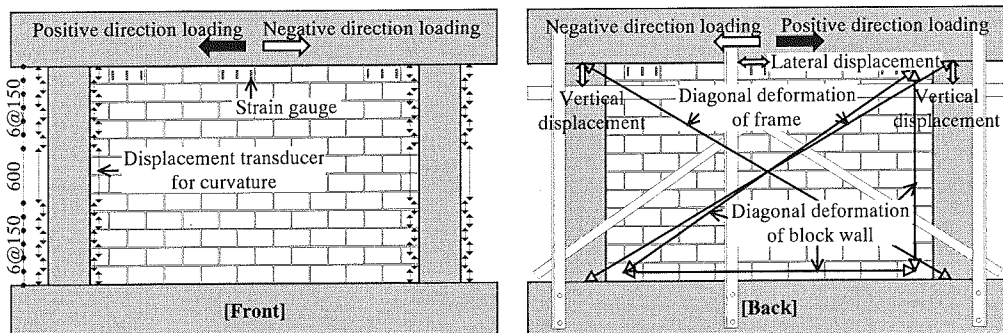
Figure 4. Loading history
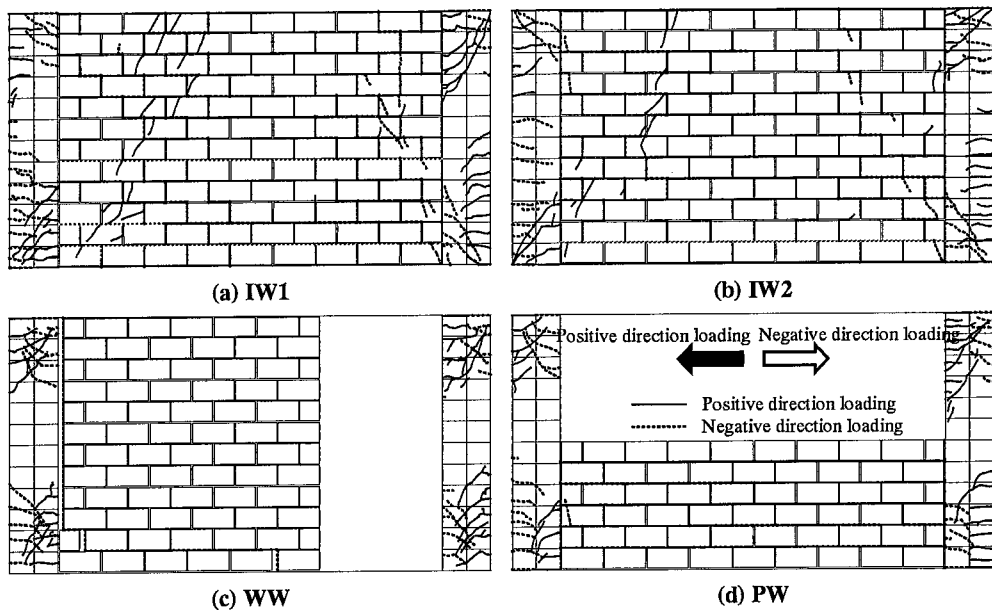
Figure 5. Measurement system

Specimen IW1

Specimen IW1 has flexural cracks in RC columns, and vertical and horizontal cracks in joint mortar between CB units at the first cycle of +0.1%. During 0.2% loading, the cracks develop and some cracks in joint mortar extend diagonally in CB units. At the first cycle of +0.4%, clear shear cracks in both columns and wider cracks in CB wall are observed although few cracks are newly found in the wall. During 0.67% loading, the flexural and shear cracks previously observed in columns significantly develop and stair-stepped diagonal cracks running through the wall center are observed. Since the shear cracks in the column bottom of compression side rapidly open at –1.5%, the test is terminated after 1.5 cycles of 1.5% loading.

Specimen IW2

Specimen IW2 has a crack pattern in both columns and wall which is almost the same as that of specimen IW1. Although the strength deterioration is observed at the first cycle of +2.0%, a rapid increase in crack width is not found. Since the shear crack in the column bottom of compression side rapidly open at +3.33%, the experiment is terminated.

Specimen WW

Specimen WW has flexural cracks in columns at the first cycle of +0.1% as is also found in specimen IW1. Since the specimen has a door opening on the right side of the frame and the CB wall end of the opening side is not directly confined by the column, stair-stepped diagonal cracks do not develop during the positive direction loading, and the whole CB wall gradually slides to the right during cyclic loading causing separation of CB units from the left side column. Since the CB wall acts as a compressive strut in specimens IW1 and IW2, both of which have no opening, stair-stepped cracks diagonally run in the wall extending through the bottom of compression column and the top of tensile column as shown in Figures 6(a) and (b). The wall of specimen WW is, however, much less confined by the boundary frame and does not contribute to the frame's lateral resistance. The specimen therefore behaves much like a bare frame and the shear cracks occur on both ends of columns simultaneously. At the first cycle of –2.0%, a shear crack in the column grows to 8 mm wide and the strength deteriorates during the following loading although it does not increase in width.

(a) IW1

(b) IW2

(c) WW

(d) PW

Positive direction loading Negative direction loading

——— Positive direction loading
·········· Negative direction loading

Figure 6. Cracks in RC columns and CB wall at the 1st cycle with peak drift angle of +1.0%

Specimen PW

Specimen PW has 2 major cracks horizontally crossing the mid-wall at 0.2%, and then the wall is divided into 3 layers of CB units. Shear cracks in the column bottom of compression side are observed at the first cycle of +0.4%. During 0.67% loading, cracks are observed in the entire bed joint (horizontal joint) of the CB wall causing slippage at the joint interface. Since the shear failure is observed simultaneously at −1.6% both in the column bottom of compression side and the column top of tension side, the experiment is terminated.

The Relation of Lateral Load and Drift Angle

Figure 7 shows the relation between the lateral load and the drift angle of each specimen. The relation of maximum strength of overall frame, load-deflection curve, and the average shear stress of CB wall in each specimen is briefly described below.

Specimen IW1

The maximum strength of 960 kN is recorded at the first cycle of +0.67% and no remarkable strength deterioration is found until 1.33%. The shear cracks at the column bottom of compression side rapidly open at −1.5%, and the lateral load carrying capacity deteriorates to about 80% of the peak value as shown in Figure 7. The load-deflection curve and crack patterns indicate that the specimen finally fails in shear due to shear force acting on the column bottom of the compression side after yield hinges are formed at both ends of the columns.

To investigate the contribution of CB wall to the lateral resistance of the specimen, the strength of bare frame is calculated and compared with test results as plotted in Figure 7, where a plastic hinge zone is assumed over a distance of D (D: column depth, 450 mm) at both ends in columns considering only the crack patterns and distributions along columns [2]. The strength of overall frame obtained from the experiment is about 1.4 times of the calculated shear strength, which agrees well with the test results of specimens WW and PW as discussed subsequently, and the CB wall greatly contributes to the frame strength if the out-of-plane failure does not occur in the wall. Assuming the discrepancy between the observed peak load and the calculated shear strength is carried by the CB wall, the average shear stress t to the sectional area A including hollow ($A = 390 \times 190$ mm) is approximately 0.4 N/mm^2.

Specimen IW2

The maximum strength of 630 kN is recorded at the first cycle of +1.0%. Although the strength deterioration is slightly observed at the first cycle of +2.0%, no remarkable strength deterioration is found until 3.33%, and the stable lateral load carrying capacity is maintained until final loading. Since the specimen has the low axial force level, it has lower strength but higher ductility than specimen IW1. The strength of overall frame obtained from the experiment is about 1.5 times of the calculated flexural strength and the average shear stress t of the CB wall is approximately 0.3 N/mm^2, if the out-of-plane failure does not occur in the wall.

Specimen WW

The maximum strength of 734 kN is recorded at −1.6%, which is far less than that of specimen IW1 having no opening but the same axial force level. As mentioned above, since the specimen has a door opening, the CB wall is much less confined by the boundary frame and does not contribute to the frame's lateral resistance. Therefore, the strength of overall frame obtained from the experiment is about 1.1 times of the calculated shear strength, which demonstrates that the specimen's behavior is similar to a bare frame and it is highly dependent on the opening configuration in wall.

Specimen PW

The maximum strength of 744 kN is recorded at −1.6% and the shear failure simultaneously occurs in the column bottom of compression side and the column top of tension side. Since the entire bed joint is through-cracked horizontally, each CB unit slides at the cracked interface. The columns are, therefore, less interacted with the CB wall and the specimen demonstrates a behavior similar to a bare frame. The strength of overall frame obtained from the test corresponds well with the calculated shear strength.
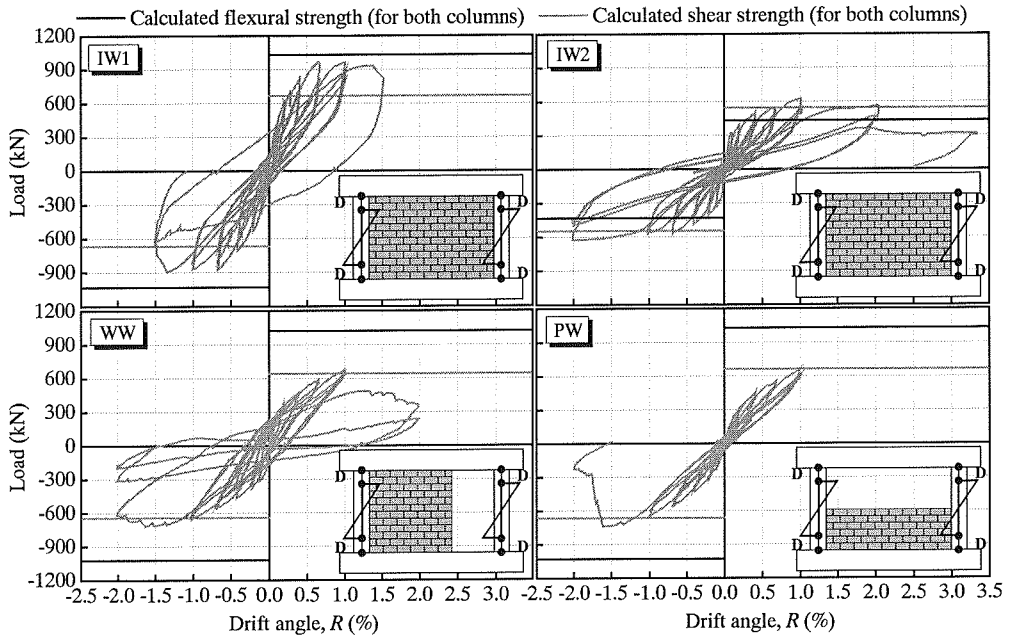
Figure 7. Load vs. drift angle of each specimen

CRACK WIDTHS AND RESPONSE OF SPECIMENS

Measurement of Crack Width

Cracks in members after an earthquake are visible and essential evidence of damage that can be found at the building site, and they often provide valuable information regarding the response that the building has experienced and its residual capacity. To investigate the relationship between damage and structural response, crack widths in RC columns and CB walls are carefully measured at peak loads and unloaded stages. Figure 8 shows the measurement points in columns and walls made in this study.

The widths of flexural and shear cracks observed at the top and bottom of each column are measured. Since crack widths are not necessarily uniform along the crack, its major width which is deemed to be largest along a crack is measured. It should also be noted that the width perpendicular to the crack is measured. All crack widths found in the specimen are measured during the first loading
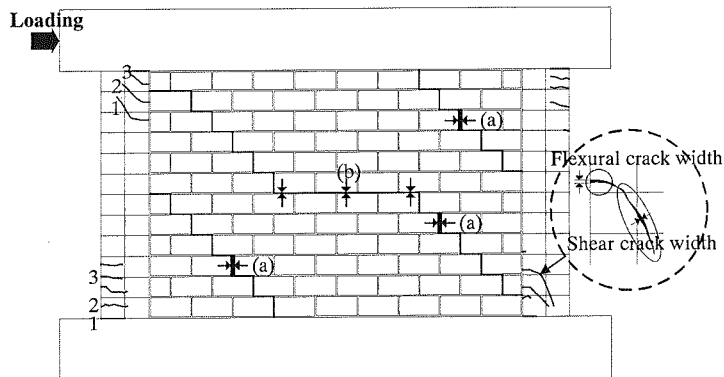

Figure 8. Schematic illustration of measured points

cycle with R smaller than 1.0%. During the second and third loading cycles with R smaller than 1.0%, and all cycles with R equal to 1.0% and larger, major 6 large cracks (3 cracks for flexure and 3 cracks for shear) are measured at both ends of each column to save crack observation time.

The widths of all stair-stepped diagonal cracks running through the wall are also measured during the first loading cycle with R smaller than 1.0%. During the second and third loading cycles with R smaller than 1.0%, and all cycles with R equal to 1.0% and larger, major wide cracks found in the head joints of one continued crack are selectively measured to record the lateral dislocation of CB units (see Figure 8(a)) while several cracks in the bed joints of one continued crack are measured to investigate a rotational behavior of wall (see Figure 8(b)). In the following sections, crack widths measured in the head joints of CB walls are investigated to understand the relationship between the observed cracks and frame's behavior.

Crack Width in CB Wall at Peak Load
The peak lateral displacement (d_p) and total crack width $(S_{max}W_p)$ in CB wall at the first cycle of positive and negative peak loads for specimens IW1 and IW2 are plotted with respect to the peak drift angle in Figure 9. In this figure, $_{max}W_p$ is defined as the maximum crack width, as is shown (a) in Figure 8, in the head joints of a continued stair-stepped diagonal crack. When the CB wall has more than one major stair-stepped diagonal crack, $_{max}W_p$ can be found along each continued crack and the sum of $_{max}W_p$ ($= S_{max}W_p$) is then calculated. Only the results in the first cycle are plotted in the figure, since minor crack widths are not measured in the subsequent second and third cycles as mentioned previously. Figure 10 shows the ratio $[S_{max}W_p / d_p]$ for specimens IW1 and IW2 with symbols "–□–". As can be found in the figures, the ratio $[S_{max}W_p / d_p]$ is approximately 0.3 and much smaller than 1.0. This reason can be explained in the following manner.

The peak lateral displacement (d_p) of frame, which is assumed identical with that of each column, can be approximately estimated as the sum of flexural deformation (d_{fp}) and shear deformation (d_{sp}) of column as shown in Figures 11(a) and (b). If each column has the identical anti-symmetrical flexural deformation and distribution as shown in Figure 11(a), no discrepancy should be found in the CB wall clear span length l_{0i} along column height. No major cracks, therefore, should be expected in the head joints under such identical deformation distribution in each column.

The shear deformation distribution in each column, however, may not be identical as shown in Figure 11(b), since the deformation due to shear cracks concentrates on the bottom of compression column and the top of tensile column resulting from a compressive strut action as can be found in specimens IW1 and IW2 (see also Figure 6). This may cause discrepancy of lateral deformation distribution in CB wall along column height. The maximum discrepancy, which may be simply expressed by the shear deformation (d_{sp}) as shown in Figure 11(b), must be absorbed by cracks in the head joints resulting in the close relationship between the shear deformation (d_{sp}) and total crack width in CB wall $(S_{max}W_p)$.
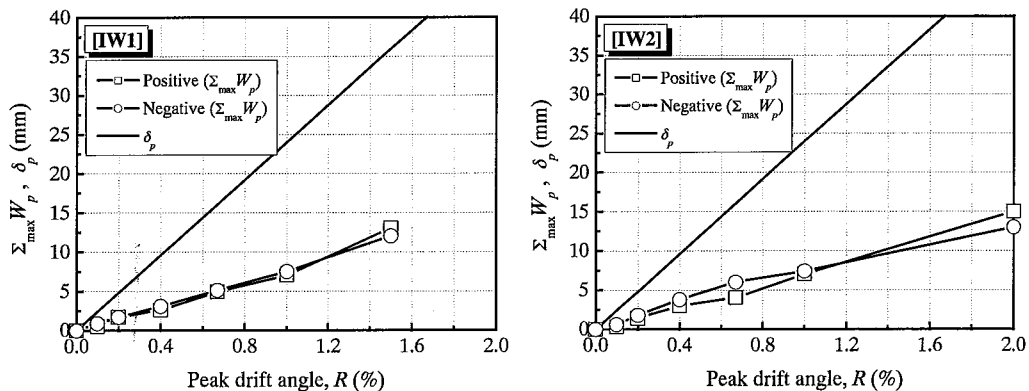

Figure 9. d_p and $S_{max}W_p$ (CB wall) vs. peak drift angle R
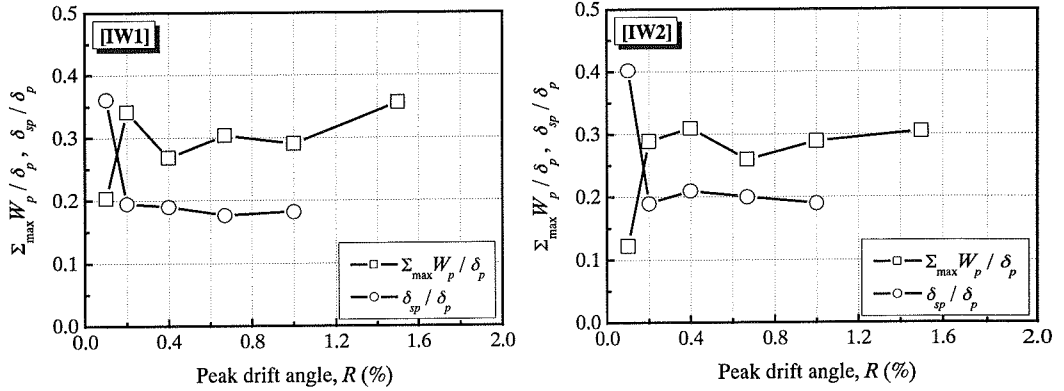
Figure 10. [$S_{max}W_p / d_p$] and [d_{sp} / d_p] (in positive loading)

(a) Flexural deformation   (b) Shear deformation
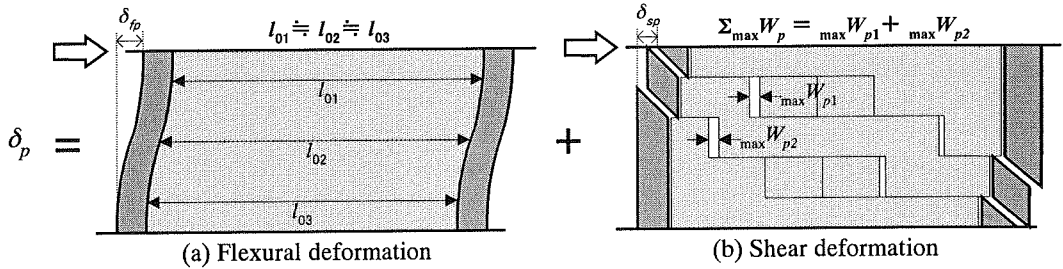
Figure 11. Deformation of column and CB wall

Figure 10 compares [$S_{max}W_p / d_p$] and [d_{sp} / d_p] of specimens IW1 and IW2, where the shear deformation d_{sp} is computed by the following equation.

$$\delta_{sp} = \delta_p - \delta_{fp}$$

where,

     d_p : peak lateral displacement measured in the tests

     d_{fp} : average value of flexural deformation in each column calculated from the measured
            curvature distribution

The ratio [$S_{max}W_p / d_p$] obtained from the crack width in CB wall slightly overestimates [d_{sp} / d_p]. This is primarily because the contribution by discrepancy of flexural deformation distribution, which results in the crack development in head joints, is included in $S_{max}W_p$ although it is neglected to simplify the discussion above. The contribution of flexural deformation distribution to crack width in CB wall will be studied in the subsequent section.

Crack Width in CB Wall at Unloaded Stage
The residual lateral displacement (d_0), total residual crack width ($S_{max}W_0$) in CB wall at the first cycle of positive and negative unloaded stages for specimens IW1 and IW2 are plotted with respect to the peak drift angle in Figure 12. The measurement method of total residual crack width ($S_{max}W_0$) and maximum residual crack width ($_{max}W_0$) in CB wall at unloaded stage is the same as that of total crack width ($S_{max}W_p$) and maximum crack width ($_{max}W_p$) at peak load.

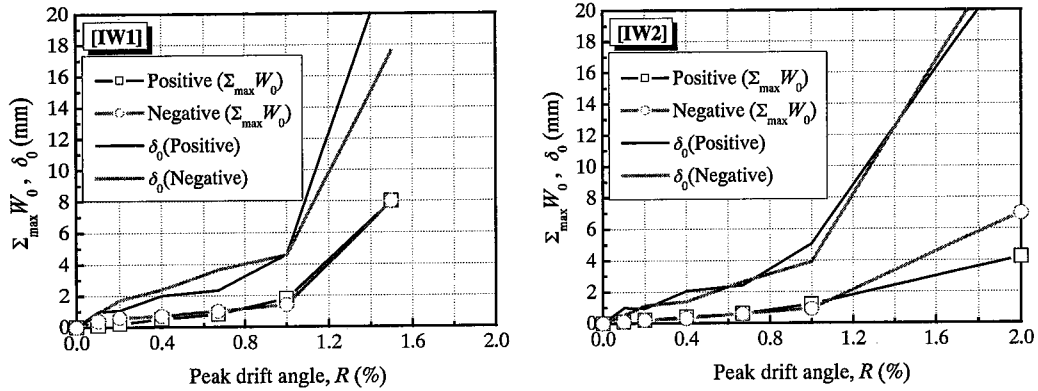As can be found in Figure 13, the ratio [$S_{max}W_0 / d_0$] for specimens IW1 and IW2 is approximately

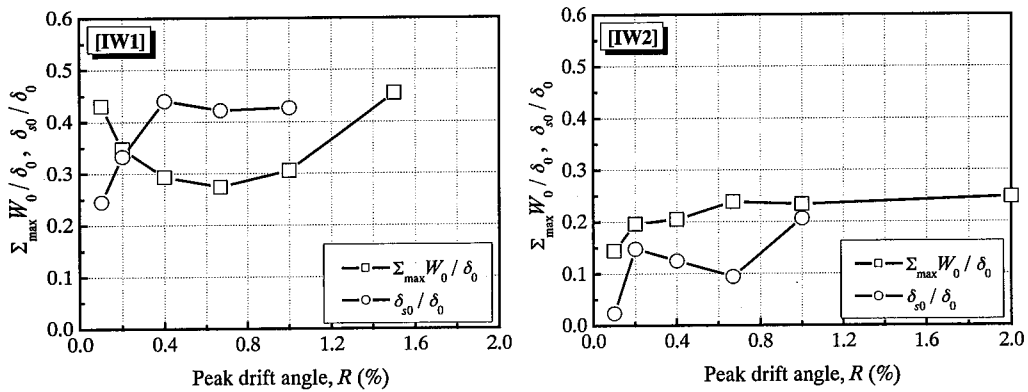**Figure 12.** d_0 and $S_{max}W_0$ (CB wall) vs. peak drift angle R

Figure 13. $[S_{max}W_0 / d_0]$ and $[d_{s0} / d_0]$ (in positive loading)

0.3, and is similar to that found in peak loading stages shown in Figure 10. It should be noted, however, that the relationship between $[S_{max}W_0 / d_0]$ and $[d_{s0} / d_0]$ is not consistent in two specimens, which may be resulted from measurement errors significantly and sensitively affecting the flexural deformation distribution computed in the small displacement range of unloaded stage.

Crack Width in CB Wall Contributed by Flexural Deformation Distribution of Column
The contribution by the discrepancy of flexural deformation distribution is neglected to estimate the crack width in CB wall in the previous discussions. In this section, the crack width in CB wall is estimated considering the discrepancy of flexural deformation distribution along each column height and compared with test results. Figure 14 illustrates the outline of the estimation procedure.

(1) Flexural deformation distribution
The distributions of flexural deformation of two RC columns along their height, $_t d_f(x)$ and $_c d_f(x)$, are computed based on the measured curvature distribution, where "t" and "c" denote "tension" side and "compression" side, and "x" denotes the distance from the top of each column, respectively.

(2) Shear deformation distribution
Assuming that the discrepancy between $d_f(0)$ and the overall lateral displacement d is shear deformation caused in the column, and that the shear deformation is linearly distributed over the top

1.5D for tension side column and the bottom 1.5D for compression side column, the shear deformation distribution can be obtained as shown below.

$$_t\delta_s(x) = (\delta -_t\delta_f(0))\cdot\frac{1.5D-x}{1.5D} \qquad (0\le x<1.5D)$$

$$= 0 \qquad (1.5D\le x)$$

$$_c\delta_s(x) = (\delta -_c\delta_f(0)) \qquad (0\le x<h_0-1.5D)$$

$$= (\delta -_c\delta_f(0))\cdot\frac{h_0-x}{1.5D} \qquad (h_0-1.5D\le x\le h_0)$$

where,

d	: lateral displacement at the top of the specimen
$_td_f(x),\ _cd_f(x)$	: flexural deformation distribution along column height
$_td_s(x),\ _cd_s(x)$	: shear deformation distribution along column height
h_0	: column clear height (=2,400 mm)
x	: distance from column top
D	: column depth (=450 mm)

(3) Column deformation distribution

The deformation distribution $d(x)$ along each column then can be written as defined below.

$$_t\delta(x)=_t\delta_f(x)+_t\delta_s(x)$$

$$_c\delta(x)=_c\delta_f(x)+_c\delta_s(x)$$

(1) Flexural deformation
distribution

(2) Shear deformation
distribution

(3) Column deformation
distribution

(4) Crack width
distribution
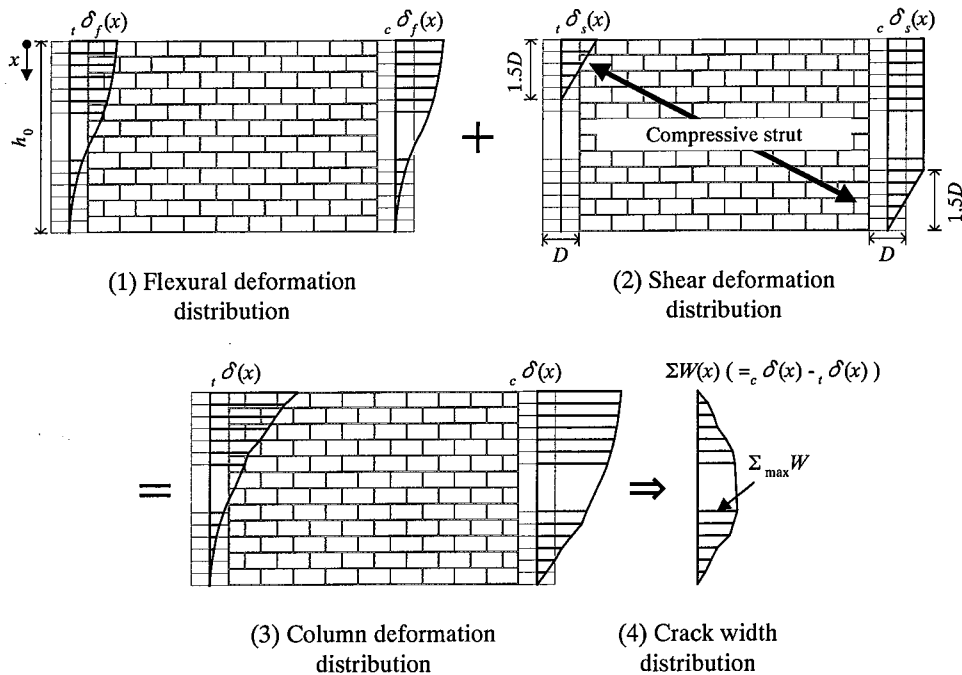
Figure 14. Deformation distribution assumed in frame

(a) $[S_{\max}W_p / d_p]$, $[d_{sp} / d_p]$ and $[_{\max}(_c\delta_p - _t\delta_p) / \delta_p]$ at peak load

(b) $[S_{\max}W_0 / d_0]$, $[d_{s0} / d_0]$ and $[_{\max}(_c\delta_0 - _t\delta_0) / \delta_0]$ at unloaded stage
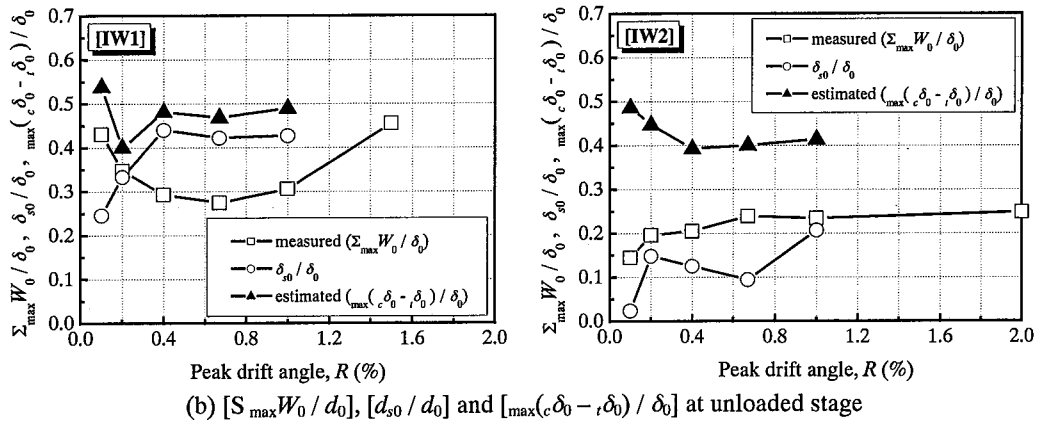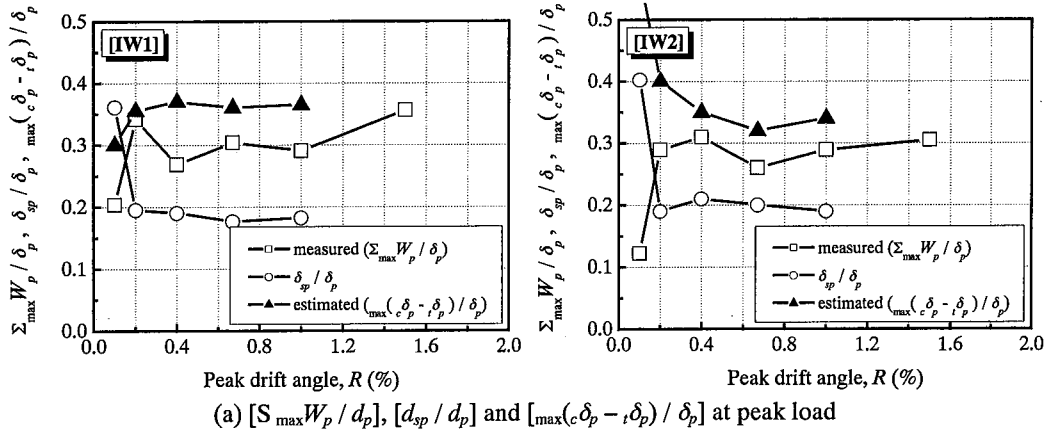
Figure 15. Comparison of crack width in CB wall

(4) Crack width distribution

Assuming that the discrepancy of deformation in two columns corresponds to the crack width in CB wall, the crack width distribution $\Sigma W(x)$ and its maximum value $\Sigma_{\max}W(x)$ can be expressed as:

$$\sum W(x) = _c\delta(x) - _t\delta(x)$$
$$\sum{}_{\max}W = {}_{\max}[\sum W(x)] = {}_{\max}\left(_c\delta(x) - _t\delta(x)\right)$$

Figures 15(a) and (b) show the results obtained from the procedure described above. The ratio $[_{\max}(_c\delta_p - _t\delta_p) / \delta_p]$ at peak loads for specimens IW1 and IW2 compared with the result of Figure 10 ($[S_{\max}W_p / d_p]$ and $[d_{sp} / d_p]$) is shown in Figure 15(a), and the ratio $[_{\max}(_c\delta_0 - _t\delta_0) / \delta_0]$ at unloaded stages compared with the result of Figure 13 ($[S_{\max}W_0 / d_0]$ and $[d_{s0} / d_0]$) is shown in Figure 15(b), respectively. The ratios $[_{\max}(_c\delta_p - _t\delta_p) / \delta_p]$ and $[_{\max}(_c\delta_0 - _t\delta_0) / \delta_0]$ are larger than $[S_{\max}W_p / d_p]$ and $[S_{\max}W_0 / d_0]$ obtained from the crack width in CB wall, respectively. Bearing in mind that all cracks developed in the specimen are not necessarily measured, $S_{\max}W_p$ and $S_{\max}W_0$ should be smaller than the actual value and the results shown in Figure 15 are therefore consistent with those expected.

Estimation of Measured Crack Width in CB Wall by Simplified Model

In the previous section, the measured crack width in CB wall is estimated based on the flexural and shear deformation distribution of each column, where the curvature distribution is taken into account.

Since the curvature distribution of column is, however, generally unknown in buildings damaged by an earthquake, a simplified model that directly estimates the crack width in CB wall is proposed, and the correlation between measured and estimated results is discussed. Figure 16 demonstrates the outline of the simplified model.

Based on studies by Maeda et al., AIJ guidelines define the relationship between residual crack width and residual deformation for RC members [3]. However, few researches on this relationship for RC frames and/or CB wall infilled frames have been yet made to date. It is therefore of great interest and significance to investigate the applicability of simplified model to CB wall infilled frames.

(a) Flexural deformation   (b) Shear deformation
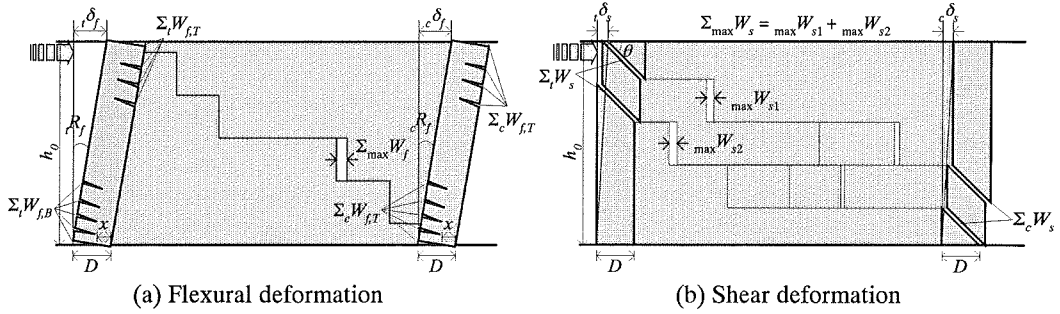
Figure 16. Simplified model of column and CB wall

(1) Crack width due to flexural deformation

The flexural deformation of two RC columns, $_t d_f$ and $_c d_f$, are computed based on the measured total flexural crack width, where "t" and "c" denote "tension" side and "compression" side of column, respectively. The flexural deformation of each column can be approximately estimated using the average total flexural crack width in top and bottom of column as shown below [3].

$$_t \delta_f = {}_t R_f \cdot h_0$$

$$= \frac{1}{D-x} \cdot \left(\frac{\Sigma_t W_{f,T} + \Sigma_t W_{f,B}}{2} \right) \cdot h_0$$

$$_c \delta_f = {}_c R_f \cdot h_0$$

$$= \frac{1}{D-x} \cdot \left(\frac{\Sigma_c W_{f,T} + \Sigma_c W_{f,B}}{2} \right) \cdot h_0$$

where,

$_t d_f$, $_c d_f$	: flexural deformation of tension and compression side column, respectively
$_t R_f$, $_c R_f$	: flexural rotation angle of tension and compression side column, respectively
$\Sigma_t W_{f,T}$, $\Sigma_t W_{f,B}$	: total flexural crack width of top and bottom in tension column, respectively
$\Sigma_c W_{f,T}$, $\Sigma_c W_{f,B}$	: total flexural crack width of top and bottom in compression column, respectively
D	: column depth (=450 mm)
x	: distance from extreme compression fiber to neutral axis (=0.2D = 90 mm)
h_0	: column clear height (=2,400 mm)

The maximum discrepancy of flexural deformation distribution of both columns, which causes the crack development in head joints as discussed earlier, is assumed in this paper to develop at the center of column height ($h_0 / 2$) as shown below.

$$\Sigma_{max}W_f = \left(\frac{\Sigma_c W_{f,B} - \Sigma_t W_{f,B}}{D-x}\right) \cdot \frac{h_0}{2}$$

where,

$\Sigma_{max}W_f$: total crack width in CB wall due to the discrepancy of flexural deformation distribution

(2) Crack width due to shear deformation

The shear deformation of two RC columns, $_t d_s$ and $_c d_s$, are computed based on the measured total shear crack width of each column. The shear deformation can be roughly obtained as shown below [3].

$$_t \delta_s = \Sigma_t W_s \cdot \cos\theta$$
$$_c \delta_s = \Sigma_c W_s \cdot \cos\theta$$

where,

$_t d_s, _c d_s$: shear deformation of tension and compression side column, respectively
$\Sigma_t W_s, \Sigma_c W_s$: total shear crack width of top and bottom in tension column, respectively
θ : angle between shear crack and horizontal direction of column

The total crack width in CB wall due to shear deformation distribution can be approximately estimated using the average total shear crack width in tension and compression side column as shown below.

$$\Sigma_{max}W_s = \frac{(\Sigma_c W_s + \Sigma_t W_s) \cdot \cos\theta}{2}$$

where,

$\Sigma_{max}W_s$: total crack width in CB wall due to the shear deformation distribution

(3) Total crack width in CB wall

Assuming that the discrepancy of deformation in two columns corresponds to the total crack width in CB wall, $\Sigma_{max}W$ can be expressed as:

$$\Sigma_{max}W = \Sigma_{max}W_f + \Sigma_{max}W_s$$
$$= \left(\frac{\Sigma_c W_{f,B} - \Sigma_t W_{f,B}}{D-x}\right) \cdot \frac{h_0}{2} + \frac{(\Sigma_c W_s + \Sigma_t W_s) \cdot \cos\theta}{2}$$
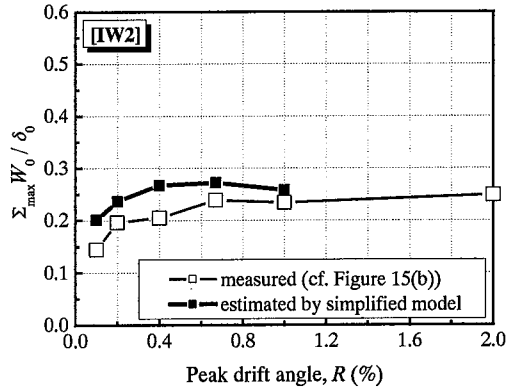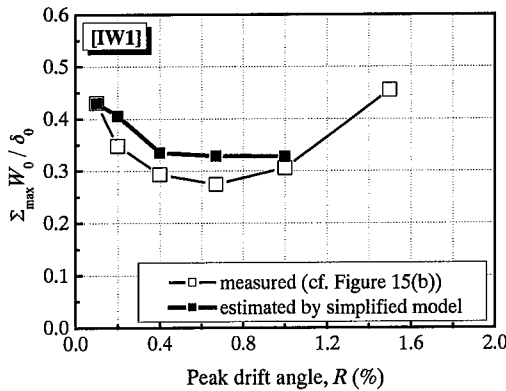

Figure 17. $[\Sigma_{max}W_0 / d_0]$ at unloaded stage

Figure 17 shows the estimated crack widths at unloaded stages obtained from the simplified model described above together with measured results. The directly measured crack widths (−□−) in CB wall compare well with the estimated results (−■−). This result implies that the simplified model proposed in this study can be applied to CB wall infilled frame.

CONCLUSIONS

Concrete block infilled RC frames for school buildings in Korea are tested under cyclic loading. The relationship between observed damage and seismic performance primarily focusing on crack width in CB walls, load bearing capacity, and residual deformation is discussed. The results can be summarized as follows.

(1) Specimens IW1 and IW2 having no opening finally fails in shear due to shear force acting on the column bottom of the compression side after yield hinges are formed at both ends of the columns. Specimen WW having a door opening behaves much like a bare frame and the shear cracks occur on both ends of columns simultaneously since the CB wall is much less confined by the boundary frame and does not contribute to the frame's lateral resistance. Specimen PW having a window opening also demonstrates a behavior similar to a bare frame since the columns are less interacted with the wall due to slippage at horizontal interface between each CB unit.
(2) The strength of overall frame in specimens IW1 and IW2 is about 1.4 and 1.5 times of the calculated strength, respectively, and the CB wall greatly contributes to the frame strength if the out-of-plane failure does not occur in the wall, while the strength in specimens WW and PW corresponds well with the calculated shear strength of a bare frame due to opening in the wall. The average shear stress t of CB wall is 0.4 and 0.3 N/mm^2 in specimens IW1 and IW2, respectively.
(3) The crack width in CB wall considering the flexural and shear deformation distribution of each column based on the measured curvature distribution is studied. The calculated values are larger than the measured. Bearing in mind that all cracks developed in the specimen are not necessarily measured, the measured values should be smaller than the actual value and the obtained results are therefore consistent with the expected.
(4) A simplified model that directly estimates the crack width in CB wall is proposed, and the correlation between measured and estimated results is discussed. The directly measured crack widths in CB wall compare well with the estimated results. This result implies that the simplified model proposed in this study can be applied to CB wall infilled frame.

ACKNOWLEDGMENT

REFERENCES

[1] The Ministry of Construction and Transportation (2002). "A study on the seismic evaluation and retrofit of low-rise RC buildings in Korea." 113-155.
[2] Architectural Institute of Japan (1988). "Standard for structural calculation of reinforced concrete structures −Based on allowable stress concept-." 167-192.
[3] Architectural Institute of Japan (2004). "Guidelines for Performance Evaluation of Earthquake Resistant Reinforced Concrete Buildings (Draft)." 155-161.